Oligomers of Poly(anhydride): Study of Interaction in Coating Binder

Anne-Cécile Lasne-Deschamps,[1] Fabienne Faÿ,[1] Olivier Sire,[2] Isabelle Linossier,[1] Karine Vallée-Réhel[1]

[1]*LBCM, EA 3884, Université de Bretagne Sud, BP92116, 56321 Lorient Cedex, France*
[2]*LIMATB, EA 4250, Université de Bretagne Sud, CER Yves Coppens BP 573, 56017 Vannes cedex, France*

Received 28 February 2011; accepted 4 July 2011
DOI 10.1002/app.35174
Published online 16 January 2012 in Wiley Online Library (wileyonlinelibrary.com).

ABSTRACT: Polyanhydrides are largely used in biomedical and pharmaceutical fields because of their biodegradability and controlled degradation. In this work, oligomers were investigated as film binders for environmental applications. To overcome the main disadvantages of polyanhydrides (low solubility in common solvents and high melting points), oligomers based on sebacic acid were prepared. Characterization was carried out by nuclear magnetic resonance and electrospray ionization to obtain chemical structures of the products. The formation of weak interactions, which confer cohesion between chains, allows film properties to be observed. The impact of the solvent polarity on the specific organization was investigated by a combination of focused methods: capillary viscosimetry, IR spectroscopy, polarized light microscopy, and X-ray diffraction. © 2012 Wiley Periodicals, Inc. J Appl Polym Sci 125: 1592–1600, 2012

Key words: coating; polyanhydrides; oligomers; self-organization; sebacic acid

INTRODUCTION

Polyanhydrides are well-known biodegradable polymers. Their surface-eroding properties in aqueous media make them desirable for the controlled release of bioactive molecules as drugs and functional tissue substitutes.[1–3] Their main advantages are the adjustability of degradation and release rates, the zero order kinetics of release, and biocompatibility.[4] The first application of polyanhydrides as a biodegradable matrix for controlled drug delivery systems was reported in 1983.[5] Since then, polyanhydrides of aliphatic and aromatic diacids have been extensively investigated as useful biomaterials for controlled drug delivery systems.[6,7] However, their low solubility in common organic solvents and their high melting points limit their potential applications, especially in environmental fields.[8–10] This is the reason why new strategies of formulation need to be considered to enlarge the use of polyanhydrides and overcome their main disadvantages. Due to environmental constraints, biodegradable coatings based on polyanhydrides should be increasingly employed in the future.

The purpose of this study is to evaluate the potential of anhydride oligomers as film-forming matrices. The use of oligomers clears up many difficulties of synthesis (which is long, extended, and tedious), stability, and solubilization. Covalent bonds are replaced by weak interactions to preserve cohesion between molecules and obtain film properties. To carry out experiments, poly(sebacic anhydride) (PSA) has been selected. Indeed, hundreds of polyanhydrides have been synthesized in the last 20 years, but only PSA and its derivatives (drug delivery system, medical devices) have been applied. Exhaustive supporting data are available.[9,11] Furthermore, PSA is a simple polymer to further study interactions between chains.

In a supramolecular system, interactions permit a stabilization of the film structure. In the literature, the most supramolecular system observed was based on hydrogen bonds.[12,13] According to the literature, hydrogen bond strength of a supramolecular system was often comparable to that of a covalent bond to least four hydrogen bonds. In this study, oligomers were based on an anhydride or carboxylic acid end group which permits the formation of hydrogen bond.

The aim of this work is to highlight the presence of interactions in the polyanhydride oligomers' film and to prove the influence of solvent properties. Evidence of organization was produced by studying coatings prepared in solvents with different properties. The selected solvents were: xylene, which is the hydrophobic, nonpolar solvent generally used for the coating formulation, and THF, which is known to break hydrogen bonds due to its high polarity.

Correspondence to: I. Linossier (isabelle.linossier@univ-ubs.fr).
Contract grant sponsor: Brittany Region.

The solvent properties influenced film organization. Many complementary techniques have been employed to highlight the variety of organizations due to different strengths of interaction. Investigations of interactions and specific organizations were carried out by IR spectroscopy, capillary viscosimetry, thermogravimetric analysis, polarized light microscopy, and X-ray powder diffraction. The study of interaction was carried out from different oligomer conditions: in solution, during drying, and in dry varnishes. Capillary viscosimetry allows for the study of the difference between solvent and chain affinity. Polarized light microscopy has shown the morphology of the crystalline phase of the samples. IR spectroscopy and X-ray diffraction have given supplementary information on the crystalline phase (crystallinity rate and amorphous index).

EXPERIMENTAL

Materials

Sebacic acid (SA; 99%, $M = 202.25$ g/mol) was purchased from Aldrich Chemical. Acetic anhydride (99+%) was purchased from Acros organic. Tetrahydrofuran (THF, HPLC grade), xylene (laboratory reagent grade), and analytical solvent were purchased from Fisher scientific. All the reactants were used without further purification.

Oligomer synthesis

From the prepolymer synthesis of Domb et al.,[8] a protocol of oligomers synthesis was determined. The PSA oligomers were prepared by polycondensation of diacid monomer and acetic anhydride with reflux at 170°C and different reaction times from 4 to 14 h (Fig. 1). The excess of acetic acid was evaporated to dryness in a rotavapor. The sample was freeze dried for one night and stored at −18°C until use. The oligomers had the consistency of a compact paste.

Methods of analysis

The molecular weight distribution of the oligomers was determined by size exclusion chromatography (SEC). It was performed on a Merck (L-7110) instrument, with a evaporating light scattering (ELS) detector (Sedex 55, Sedere). Samples were eluted in THF through a polystyrene/divinylbenzène (PL) gel column (Varian, mixed-D 5µm pore size) at a flow rate of 1 mL/min. Molecular weight of oligomers was determined relative to polystyrene standards (Varian, molecular range 580–188,700 g/mol).

Different masses of sample were detected by electrospray ionization ion trap mass spectrometry (ESI-MS) using a Bruker Esquire-LC spectrometer (Bruker

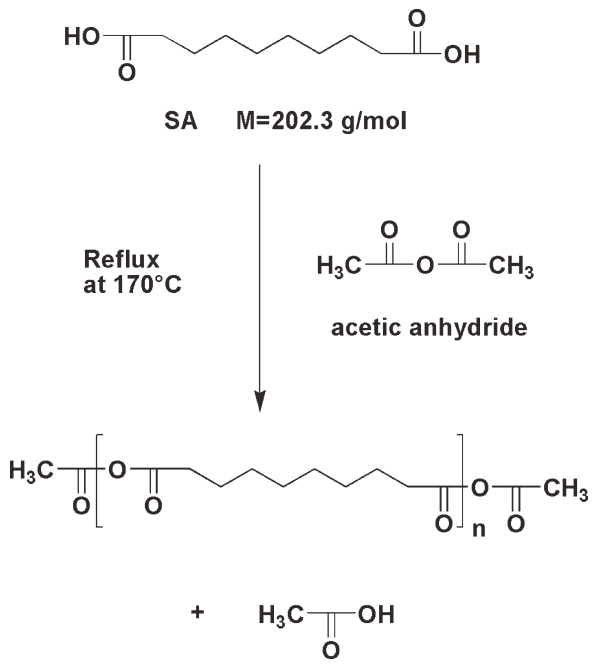

Figure 1 P(SA) oligomers synthesis.

Daltonic, Germany) under negative-ion conditions. Oligomers were put in solution in acetonitrile (ACN) and studied in direct injection at a flow rate of 2 mL/h. Capillary entrance voltage was set to 3.8 kV and dry gas temperature to 150°C. The software used was Bruker Data Analysis.

For the solubility test, the sample was placed in xylene and agitated to dissolve. The resulting solution was placed in rotavapor to remove the solvent. Then, samples were placed in vacuum desiccators for 24 h and weighed. The measurement was repeated three times.

^{1}H and ^{13}C-NMR spectra were recorded at room temperature in DMSO solvent on a Bruker Advance 400 photometer at 400 MHz. Chemical shifts are given in ppm relative to tetramethylsilane. The oligomers had typical aliphatic group at 1.25 ppm (s, 8H, —CH_2—($C\mathbf{H}_2$)$_4$—CH_2—), 1.5 ppm (d, 4H, —CH_2—$C\mathbf{H}_2$—(CH_2)$_4$—$C\mathbf{H}_2$—CH_2—), 2.2 ppm (s, 6H, $C\mathbf{H}_3$—CO—O—CO—CH_2—CH_2—(CH_2)$_4$—CH_2—CH_2—CO—O—CO—$C\mathbf{H}_3$), and (s, 4H, CH_3—CO—O—CO—$C\mathbf{H}_2$—CH_2—(CH_2)$_4$—CH_2—$C\mathbf{H}_2$—CO—O—CO—CH_3), 2.5 ppm (DMSO). ^{13}C-NMR verified the ^{1}H-NMR structure: 22 ppm ($\mathbf{C}H_3$—CO—O—CO—CH_2—), 23.6 ppm (CH_3—CO—O—CH_2—$\mathbf{C}H_2$—CH_2—(CH_2)$_2$—CH_2—CH_2—CH_2—CO—), 24.46 ppm (OH—CO—CH_2—$\mathbf{C}H_2$—CH_2—(CH_2)$_2$—CH_2—CH_2—CH_2—CO—O—CH_3), 28 ppm (CH_3—CO—O—CO—CH_2—CH_2—$\mathbf{C}H_2$—(CH_2)$_2$—$\mathbf{C}H_2$—CH_2—CH_2—CO), 28.4 ppm (CH_3—CO—O—CO—CH_2—CH_2—CH_2—($\mathbf{C}H_2$)$_2$—CH_2—CH_2—CH_2—CO—), 33.6 ppm (OH—CO—$\mathbf{C}H_2$—CH_2—CH_2—(CH_2)$_2$—CH_2—CH_2—CH_2—CO—O—CO—CH_3), 34.4 ppm (CH_3—CO—O—CO—$\mathbf{C}H_2$—CH_2—CH_2—(CH_2)$_2$—CH_2—CH_2—$\mathbf{C}H_2$—CO—O—CO—CH_3), 167.1 ppm (CH_3—$\mathbf{C}$O—O—

CO—CH_2—), 169.7 ppm (CH_3—CO—O—**C**O—CH_2—), 172.2 ppm (OH—**C**O—CH_2—).

Thermal analysis was conducted by differential scanning calorimetry (DSC) using a Perking–Elmer calorimeter. Four to five milligrams PSA samples were analyzed from −70 to 50°C with a heating rate of 20 °C/min (first scan). Samples were slowly cooled from 50°C to −70°C with a cooling rate of 5 °C/min. The second scan was made at 20 °C/min from −70 to 50°C. The DSC analysis of coatings required a different program. The coating samples were scanned from 0 to 100°C with a heating rate of 20 °C/min (first scan). Samples were slowly cooled from 100 to 0°C. The second scan was performed at 20 °C/min from 0 to 100°C. The melting temperature (T_m) was plotted in the second scan.

Viscosity of the different solutions was determined by an Ubbelohde-type viscosimeter, thermostated at 25°C, using THF and xylene as solvent.

IR was performed in the attenuated total reflection (ATR) mode by using a Bruker Spectrum Tensor 27 system equipped with an ATR cell with a diamond reflection element. Samples were applied directly onto the surface of ATR crystal. Spectra result from the accumulation of 16 scans at 4 cm^{-1} resolution. The wavenumber range was 4000–400 cm^{-1}.

The surface deposits were investigated by polarized light microscopy using a LEICA DMLP microscope. The deposits were transferred onto a glass slide and covered with a coverslip. The sample was melted at 70°C and observed during cooling to the ambient temperature.

Coatings were based on a 50 : 50 (w:w) blend of PSA oligomers and solvent. For studies, PSA coatings were deposited on a glass strip and scratched out after drying in vacuum desiccators.

Crystallinity rate was determined from X-ray diffraction on powder using a FR591 Bruker AXS-X-ray generator with monochromatic CuKα radiation (λ = 1.54 Å) and linear collimation. Samples were studied at an angle of $0° < 2\theta < 40°$ and the detector was positioned at 170 mm.

RESULTS AND DISCUSSION

Synthesis/characterization

Optimization of synthesis conditions

The goal of this study was to produce oligomers using a quick reaction while maintaining a control over the chain length. The first results have shown that the optimum length of chains was estimated at 3–4 repeat units to obtain solubility in xylene and stability before use. Indeed, the smaller the chain, the more soluble the oligomers. The synthesis was performed during different reflux times (4, 6, 8, and 14 h). The corresponding oligomers were first characterized by an SEC and solubility test. Table I sums up the variation of M_w measured by the SEC as a function of time reaction. It can be seen that M_w increases with reaction time. For example, for 14 h of reaction time, M_w of 1000 g/mol was obtained, corresponding to a number of repeat units per chain of 5–6, whereas for 8 h of reaction, the M_w was 900 g/mol and the number of units per chain was 4–5. Nevertheless, for 4 and 6 h of reaction, the same M_w was obtained (M_w = 700 g/mol). Indeed, the longer the reaction time, the less soluble the oligomers. Four hours (PSA-1) corresponds to a better solubility, so the analysis was carried out with PSA-1.

TABLE I
Variation of M_w, Unit Number, and Solubility in Function to Reaction Time

	Reaction time (h)	M_w[a] (g/mol)	Units number[b]	Solubility in xylene (g/L)
PSA-1	4	700	3–4	90
PSA-2	6	700	3–4	46
PSA-3	8	900	4–5	30
PSA-4	14	1000	5–6	20

[a] Determined by SEC (THF, PS standard).
[b] Determined by ESI–MS.

Characterization of oligomers PSA-1

Oligomers were characterized by several methods:

NMR, SEC, and electrospray ionization (ESI) studies have produced structural information and molar masses of the oligomers.

Thermal properties and crystalline forms were studied from DSC and IR, respectively.

The ^{1}H-NMR spectrum of polyanhydride oligomers exhibited a typical peak at 2.2 ppm which corresponds to anhydride function.[14] No acid peak was observed in ^{1}H-NMR. ^{13}C-NMR spectrum corroborated the ^{1}H-NMR structure. The main peaks were 22 ppm ($\mathbf{C}H_3$—CO—O—CO—CH_2—) and 172.2 ppm (OH—**C**O—CH_2—). These results confirmed the presence of anhydride and acid terminal groups. All of the experimental data revealed the presence of anhydride groups in the middle of the oligomers chain and at the extremity of the chain. Despite molar weight and degree of polymerization, the desired structure (anhydride function) was obtained. Furthermore, NMR studies revealed a small remaining amount of acetic acid at 21 ppm ($\mathbf{C}H_3$—CO—OH) and 174.5 ppm (CH_3—**C**O—OH). The presence of acetic acid was required to make oligomers' solubilization easier (results not shown). This is the reason why the oligomers were never completely dried before their use in the preparation of the coating.

As well as the NMR analysis, mass spectra confirmed the formation of anhydride bonds in the

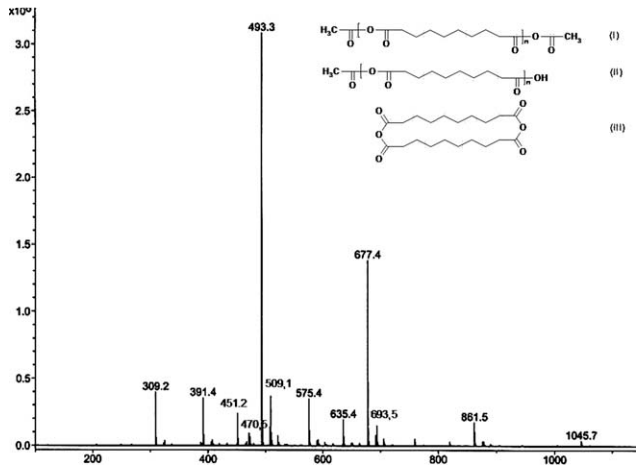

Figure 2 Structural characterization of PSA-1 oligomers by ESI (mass spectroscopy) in positive mode.

oligomers. Figure 2 features the ESI spectrum in the positive mode of the oligomers PSA-1 obtained. The mass spectrum was used to identify the different structures which coexist in the sample. Three different structures can be distinguished, called I, II, and III. They differ in the presence of linear or cyclic chains and in the presence of one or two anhydride end groups. The mass range (*m/z*) extended from 309.2 uma to 1045.7 uma which corresponds to a DPn varying from 1 to 5. The cyclic structure III is due to an intramolecular transesterification reaction and leads to corresponding peaks located at $m/z = 391.4$ and 575.4.[15] The other structures are linear chains with two anhydrides end groups I or one anhydride and one acid end group II. Despite the fact that few terminal acid and cyclic structures were present in the oligomers, the desired structure (I) is mainly observed. Moreover, mass analysis demonstrates that several lengths of oligomers chains coexist. In fact, synthesis of small length chain brings about a high structural polydispersity.

In conclusion, SEC normally showed the distribution of chain lengths (polydispersity) and molar mass in polymer. Standard polystyrene calibration did not allow for accurate values and seemed to overestimate masses ($M_w < 689$ g/mol). Indeed, the SA monomer mass was outside the calibration curve of PS standard. ESI displayed a distribution of chains and the accurate masses present in the oligomers; however, the ionization process did not allow for asserting that all the structures were ionized. Seeing that a comparison between the intensity is difficult, the polydispersity index could not be calculated although the observed values were close to what could be expected.

FTIR was also used to study the different functional groups in the oligomers. The assignment of PSA-1 peaks has already been described in the literature.[16,17] The authors demonstrated the presence of two stretching bands in the carbonyl region due to asymmetrical and symmetrical anhydride's carbonyl stretching mode. The two characteristic anhydride peaks was identified at 1813 and 1741 cm^1 in pure PSA-1 oligomers representing the SA-SA diads (Fig. 3). SA monomer and oligomers FTIR spectra were compared. In the oligomers spectrum, the methylene peak was observed in the 3400–2400 cm^{-1} region. This technique gave rise to the formation of an anhydride group in the oligomers by synthesis. There are four additional peaks directly connected with the crystallinity of the oligomers and can be attributed as follows: the 1286 and 1307 cm^{-1} bands are characteristic of the crystalline regions of the SA–SA diads and 1360 and 1386 cm^{-1} bands are characteristic of the SA–SA diads in both amorphous and crystalline region.

DSC determined the transition temperature of the oligomers. Melting temperature of PSA was given in literature.[18–22] It was 68–82°C in function of structure and masse. The sample undergoes several exothermic and endothermic transitions within the −20 to 50°C temperature range. The presence of several peaks means that several populations linked to heterogeneous chemical functions and/or intermolecular interactions coexist. Moreover, as the sum of exothermic peak areas is equal to the endothermic ones, it can be concluded that these peaks feature melting and crystallization points of these different populations.

Study of interactions

Solution of oligomer

Interaction between chains was studied in two different solvent (THF and xylene) in solution by viscosimetry and in coating by IR and light microscopy.

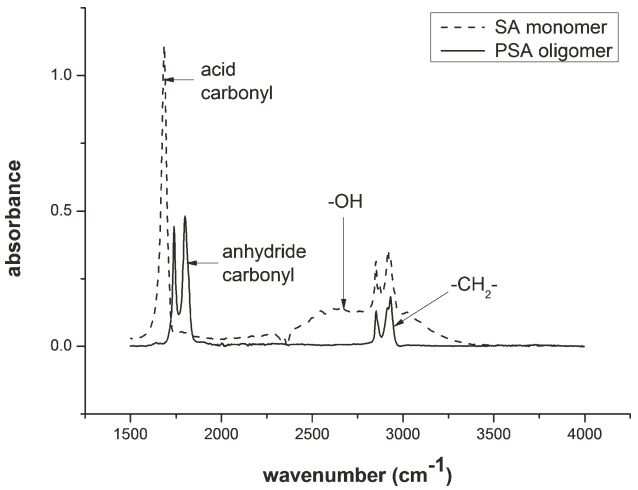

Figure 3 FTIR spectra of SA monomer and PSA-1 oligomers in the ATR mode.

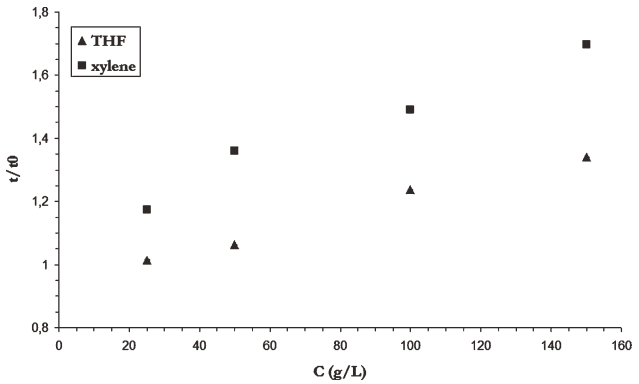

Figure 4 Reduced viscosities of PSA-1 oligomers solutions in THF and xylene.

Coatings were prepared from a 50 : 50 (w : w) blend of oligomers and solvent. This solution was called varnish.

Two solvents were used: xylene (polarity = 2.5) which is relatively apolar and so could favor interactions between chains and THF (polarity = 4.0) which is known to break hydrogen bonding.[23,24] The less polar was the solvent, the stronger were the interactions. Viscosities of oligomers solutions were measured by capillary viscosimetry to bringing to light intermolecular interactions. Solutions with varying oligomer concentrations were studied by capillary viscosimetry which permitted to determine the intrinsic viscosity of varnishes. Intrinsic viscosity was estimated from the *y*-intercept of reduced viscosity curves as a function of oligomers concentration in THF and xylene.[25] According to the viscosity curve, intrinsic viscosity was a little greater in xylene ($[\eta]_{P(SA)xylène} = 7.1\ 10^{-3} \pm 1\ 10^{-5}$ L/g) than in THF ($[\eta]_{P(SA)THF} = 10^{-4} \pm 5\ 10^{-5}$ L/g). According to Abed et al.,[26] the lower the polarity of solvent, the stronger the hydrogen bonding. Thus, according to the authors, solvent polarity influences the oligomers viscosity. Knowing that the viscosity of THF and xylene are 0.55 and 0.61 cP respectively, it can be concluded that the difference of intrinsic viscosity was not due to solvent viscosity. As seen in Figure 4, the reduced viscosities of the xylene solution are higher than THF ones. This difference is mainly explained by stronger interactions between chains in xylene than in THF. As seen previously, a lower solvent polarity led to stronger interactions. This hypothesis is confirmed by the determination of the interaction parameter χ_{12}.

$$\chi_{12} = \frac{V_1}{RT}(\delta_1 - \delta_2)^2 \quad (1)$$

With V_1° the molar volume of solvent (V_{xyl} = 120.3 and V_{THF} = 81.4 cm^3/mol), T the temperature (K), R = 8.314 J/mol, δ_1 solubility of solvent (δ_{xyl} = 18.2 and δ_{THF} = 19.4 (J/cm^3)$^{1/2}$) and δ_2 solubility of polymer. Because polymer parameter solubility was not known, Van Krevelen method was used to determine δ_2.[27]

TABLE II
Van Krevelen Method Data to Calculate δ_2

Structures	F_{di} (J$^{1/2}$ cm$^{3/2}$/mol)	F_{pi} (J$^{1/2}$ cm$^{3/2}$/mol)	E_{hi} (J/mol)
-CH_3	420	0	0
-CH_2-	270	0	0
-CO-	290	770	2000
-COO-	390	490	7000
1 plane of symmetry	–	0.5x…	_

$$\delta_2^2 = {\delta_d}^2 + {\delta_p}^2 + {\delta_h}^2 \quad \delta_d = \frac{\sum Fdt}{V}$$
$$\delta_p = \frac{\sqrt{\sum F^2}pt}{V} \quad \delta_h = \frac{\sqrt{\sum E}ht}{V} \quad V = \frac{Mn}{\rho} \quad (2)$$

With: δ_d dispersive forces component, δ_p polar forces component, δ_h hydrogen bond component, V molar volume of polymer (cm^3/mol), and ρ molar density of polymer. All components were calculated from polymer structure (Table II). It was approximated that only anhydride groups were present. These calculations show that THF has more affinity with oligomers chains (χ_{12} = 6.01) than xylene (χ_{12} = 10.53), thus preventing interactions between chains of oligomers.

During drying

First, drying varnish was studied with thermogravimetric analysis (TGA) (Fig. 5). THF ($T_{m\ exp}$ = 60°C) is more volatile than xylene ($T_{m\ exp}$ = 120°C).

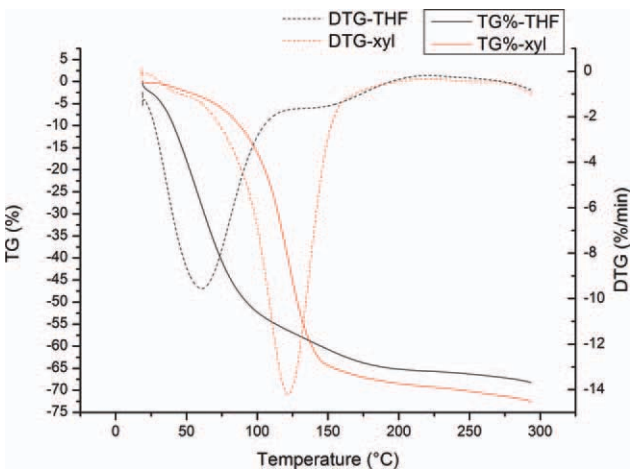

Figure 5 TGA of PSA-1 varnishes in THF and xylene. [Color figure can be viewed in the online issue, which is available at wileyonlinelibrary.com.]

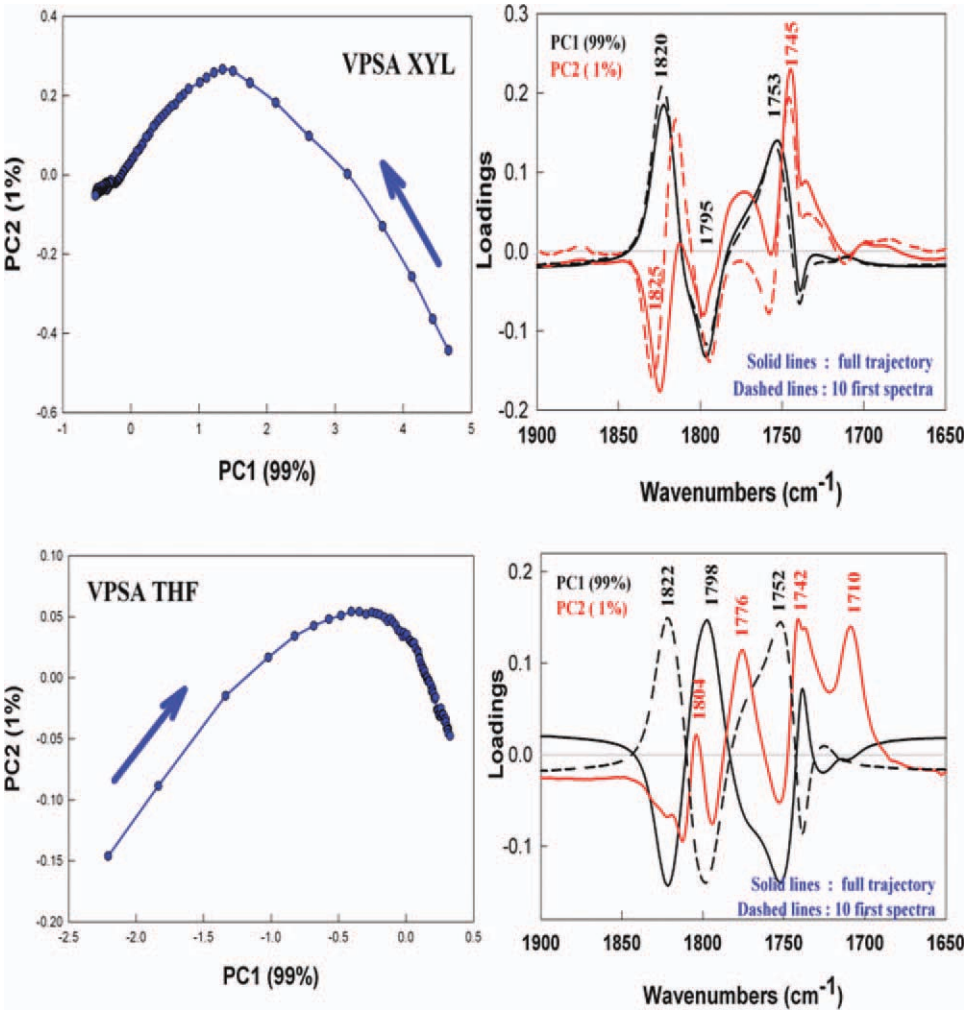

Figure 6 PCA of PSA varnishes prepared in xylene and THF. Left figures represent 2D factorial map and right figures represent statistic variable. Complete path is represented by full line and first ten points by dash line. [Color figure can be viewed in the online issue, which is available at wileyonlinelibrary.com.]

According to literature, more volatile solvent, more oligomer chains are likely to auto-assembled.[28] Moreover, loss mass analysis shows a significant difference between varnish. Indeed, varnish in THF contained appreciatively more 10% than varnish in xylene. So, some solvent molecules of THF remained traped in film which is in correlation with the χ_{12} calculated. So, it was supposed that THF molecules were responsible to the less interaction than film in xylene.

Second, organization during drying was also studied by infrared spectroscopy. More important variation was observed in the domain of anhydride frequencies. To obtain more information from these spectra, a principal components analysis (PCA) was performed. Figure 6 (left) shows the 2D factorial map. Figure 6 (right) displays the corresponding principal components which feature 99 and 1% of the total variability, respectively. PCA was carried out on complete course and on first ten points for distinguishing drying phase to the other phenomenon. First points correspond to solvent evaporation. Varnish in xylene present two near components which suggest progressive organization during drying. Varnish in THF presents two clearly opposed evolution, which the first corresponds to the solvent evaporation. So this analysis shows the importance of the solvent volatility in the organization of the film. In a volatile solvent, the mobility of chains was more reduced which is responsible to a lower crystallization.

Dry coating

To characterize the crystallinity of PSA coatings in xylene or THF, MIR spectroscopy was used. Figure 7 displays the two corresponding spectra in the 1800–700 cm^{-1} frequency domain. Regarding the discrimination between crystalline and amorphous domains, two distinct frequency domains are

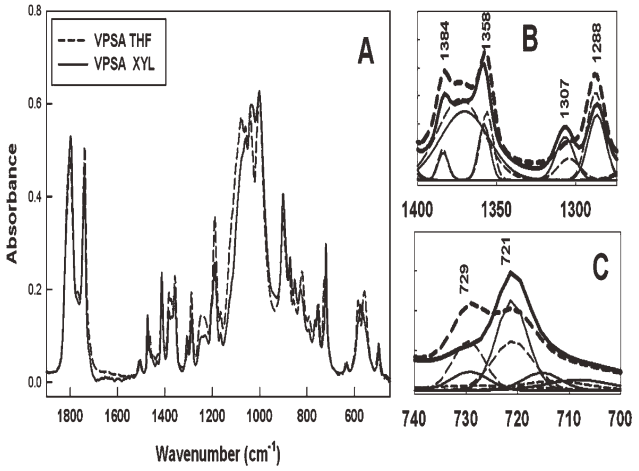

Figure 7 MIR spectra of PSA-1 coatings dissolved and dried in THF and xylene. Frame (A) features the MIR spectra of PSA coatings in the 1800–700 cm^{-1} spectral domain. To assess the crystallinity of the samples, the 1400–1260 cm^{-1} (B)) and (C) 740–700 cm^{-1} domains have been subject to spectral decomposition to estimate the area of the bands which have been reported as dependant on the polymer crystallinity. Xylene, solid line; THF, short dash lines. In (B) and (C) frames, thick lines feature the band envelopes whereas the thin lines feature the underlying spectral components.

relevant: the 1400–1250 cm^{-1} and 740–700 cm^{-1}domains. A previous study[16] has shown that the peaks located at 1382, 1360, 1307, and 1286 cm^{-1} appear only in pure PSA polymer, but not in the monomer IR spectra; as a consequence they must reflect the polymer conformations. The same authors were able to assess that the peaks at 1307 and 1286 cm^{-1} are characteristic of the crystalline region of the SA–SA dyads while the peaks at 1382 and 1360 cm^{-1} are more characteristic of the SA–SA dyads in both amorphous and crystalline regions. This spectral domain was hence subjected to spectral decomposition [see Fig. 7(B)] to compute the areas of these four bands. Following, an "amorphous index" AI was calculated as:

$$\mathrm{AI} = \frac{A_{1382} + A_{1360}}{A_{1307} + A_{1286}} \tag{3}$$

It appears that PSA-1 coatings in xylene present a smaller AI (0.478) than in the THF solvent (0.545) suggesting a higher crystallinity in xylene as compared to THF. The second domain to which attention was paid was the 740–700 cm^{-1}. Indeed, the 720/730 cm^{-1} doublet, assigned to the CH_2 rocking mode, has been previously observed to vary with strains within the polymer.[29] Transition moments of the 730 and 720 cm^{-1} vibration are parallel to the *a*-axis and the *b*-axis, respectively. These authors have observed that the asymmetry in the intensity of this doublet was caused by the preferential orientation of the *b*-axis parallel to the surface of the drawn film. Hence, the 730/720 cm^{-1} doublet provides a spectral marker of the vibrators orientations. As shown in the Figure 8(C) (and Table III) in this spectral range, the xylene PSA coating IR spectrum is dominated by a peak at 721 cm^{-1} along with a weak shoulder at 729 cm^{-1}. The same polymer in THF is characterized by two bands of roughly equal contributions with no significant spectral shifts. A weak band located at 715 cm^{-1} also appears in both samples. Hence the PSA-1 coatings exhibit a large A_{720}/A_{730} ratio (6.6) in xylene whereas this ratio decreases down to 1.2 in

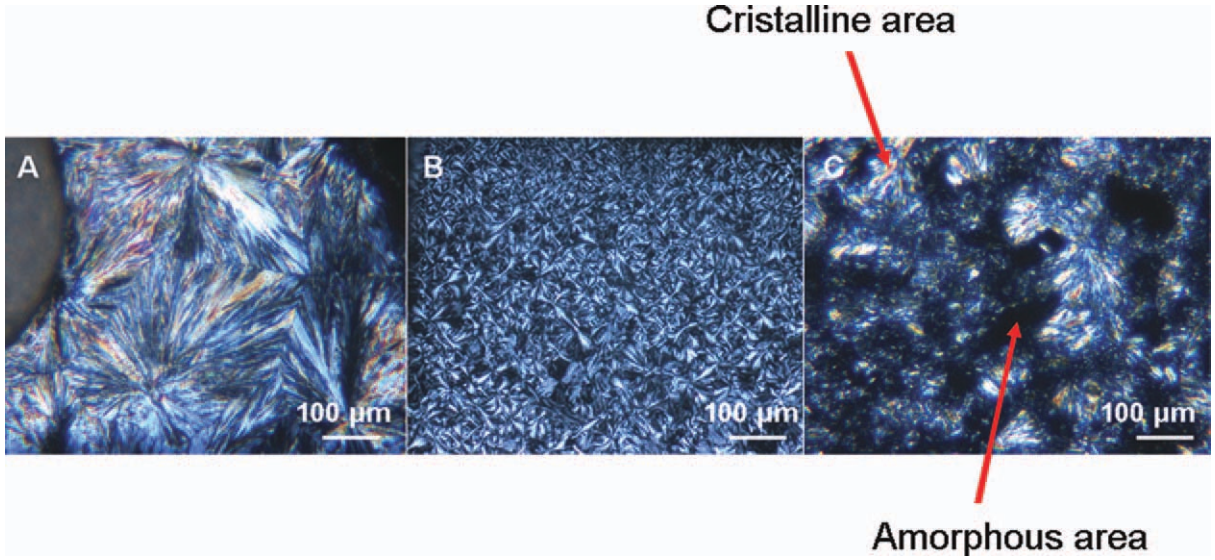

Figure 8 Polarized microscopy (20×), observation of PSA-1 (A) P(SA) oligomers; (B) P(SA) coating in xylene; (C) P(SA) coating in THF during crystallization. The scale is given by the ban at the upper right corner which is 50 µm. [Color figure can be viewed in the online issue, which is available at wileyonlinelibrary.com.]

TABLE III
Bands Assignment and Relative Areas in the 740–700 cm^{-1} Domain

Assignment		CH_2 rocking vibrations	
		b-axis	*a*-axis
Band location	715 cm^{-1}	721 cm^{-1}	729 cm^{-1}
THF	15%	47%	38%
Xylene	15%	73%	11%

the THF solvent. These findings further support that the oligomers exhibit highly ordered (anisotropic) conformations in xylene as compared to those observed in THF for which a quasi statistical (isotropic) distribution is observed.

Polarized light microscopy was used in the literature to observe the organization and morphologies of crystalline areas in the oligomers.[30,31] Göpferich et al. demonstrated that PSA polymer has a distinct microstructure like Maltese crosses spherulites.[30] Figure 8 shows the difference of the crystallization behavior of PSA-1 oligomers and varnishes prepared in xylene and THF. In PSA-1 oligomers, large spherulites organization was observed with a size of 380 μm. This revealed a complex organization: crystalline phases are organized in spherulites. In varnish prepared in xylene, lamellar structure (35 μm) was observed. These complex organizations are probably due to hydrogen interactions as observed by optical microscopy in varnish prepared in xylene and in oligomers. Varnish prepared in THF presented smaller crystallites in amorphous matrix that confirmed the absence of intermolecular organization as is explained in the literature.[31] Light microscopy was in agreement with MIR observation.

The crystallinity of oligomers was also studied by X-ray diffraction. Lahrouni and Arman[32] carried out the crystallinity rate (X_c) with crystallinity area (A_c) and amorphous area (A_a). Like the authors, X_c was calculated from the equation:

$$X_c = \frac{A_c}{A_c + A_a} \quad (4)$$

PSA-1 oligomers have a high crystallinity rate (X_c = 80.6). As seen by light microscopy, both varnishes were not of the same organization. Indeed, X-ray confirmed the last studies that is to say, varnish prepared in xylene has higher crystallinity rate (X_c = 49,4) than varnish prepared in THF (X_c = 40,8). These results confirmed light microscopy and MIR results, that is, the difference of crystallinity in function of solvent used. Indeed, the addition of solvent decreases PSA oligomer's crystallinity. Cristallinity in THF decreases more than xylene because of ability to breack interactions.

CONCLUSIONS

PSA-1 oligomers characterization has shown different structures which lead to important polydispersity. The principal structure observed is composed of linear chains with anhydride terminal group but structure composed of acid terminal group was also present in oligomer. Cristallinity studies have highlighted a difference of coating organization which depends on solvent. A more important cristallinity was observed in xylene probably due to presence of hydrogen bond formed from acid terminal groups. Coating prepared in THF present less crystallinity due to a rest of THF molecules which was opposed to the formation of interaction. Interaction control is significant in handling coating erosion to application in marine coating.

The authors thank L. Taupin for the ESI measurements, I. Pillin for the DSC analysis, F. Peresse for polarized light microscopy, N. Kervarec for RMN analysis in Brest, and C. Meriadec for X-ray measurements in Rennes.

References

1. Domb, A. J.; Langer, R. Macromolecules 1989, 22, 2117.
2. Uhrich, K. E.; Cannizzaro, S. M.; Langer, R. S.; Shakesheff, K. M. Chem Rev 1999, 99, 3181.
3. Griffin, J.; Carbone, A.; Delgado-Rivera, R.; Meiners, S.; Uhrich, K. E. Acta Biomater 2010, 6, 1917.
4. Krasko, M. Y.; Shikanov, A.; Ezra, A.; Domb, A. J. J Polym Sci Part A: Polym Chem 2003, 41, 1059.
5. Rosen, H. B.; Chang, J.; Wnek, G. E.; Linhardt, R. J.; Langer, R. Biomaterials 1983, 4, 131.
6. Guo, W.-X.; Shi, Z.-L.; Liang, K.; Chen, X.-H.; Li, W. Polym Degrad Stab 2006, 91, 2924.
7. Almudena, P.; Ashley, L. C.; Jeremy, G.; Kathryn, E. U. Macromol Rapid Commun 2009, 30, 1101.
8. Domb, A. J.; Gallardo, C. F.; Langer, R. Macromolecules 1989, 22, 3200.
9. Anastasiou, T. J.; Uhrich, K. E. Macromolecules 2000, 33, 6217.
10. Dechy-Cabaret, O.; Martin-Vaca, B.; Bourissou, D. Chem Rev 2004, 104, 6147.
11. Kumar, N.; Langer, R. S.; Domb, A. J. Adv Drug Deliv Rev 2002, 54, 889.
12. Lehn, J.-M. Prog Polym Sci 2005, 30, 814.
13. Huang, F.; Nagvekar, D. S.; Zhou, X.; Gibson, H. W. Macromolecules 2007, 40, 3561.
14. Ron, E.; Mathiowitz, E.; Mathiowitz, G.; Domb, A.; Langer, R. Macromolecules 1991, 24, 2278.
15. Domb, A. J.; Langer, R. J Polym Sci Part A: Polym Chem 1987, 25, 3373.
16. Mathiowitz, E.; Kreitz, M.; Pekarek, K. Macromolecules 1993, 26, 6749.
17. Wenig, R. W.; Schrader, G. L. J Phys Chem 1987, 91, 1911.
18. Shimon Ben-Shabat, E. A.; Raziel, A.; Domb, A. J. J Polym Sci Part A: Polym Chem 2003, 41, 3781.
19. Nagata, M.; Ioka, E. React Funct Polym 2005, 63, 163.
20. Shen, E.; Kipper, M. J.; Dziadul, B.; Lim, M.-K.; Narasimhan, B. J Controlled Release 2002, 82, 115.
21. Wen-Chuan, L.; Chu, I.-M. J Biomed Mater Res Part B: Appl Biomater 2008, 84, 138.
22. Dong, A.-J.; Zhang, J.-W.; Jiang, K.; Deng, L.-D. J Mater Sci: Mater Med 2008, 19, 39.

23. Wirtheim, E.; Avram, L.; Cohen, Y. Tetrahedron 2009, 65, 7268.
24. Binder, W. H.; Bouteiller, L.; Brinke, G. T.; Ikkala, O.; Rotello, V. M.; Ruokolainen, J.; Srivastava, S.; Xu, H.; Zirbs, R. Hydrogen Bonded Polymers, Springer: Berlin, 2007.
25. Zhu, P. W. Eur Polym J 1995, 31, 659.
26. Abed, S.; Boileau, S.; Bouteiller, L. Polymer 2001, 42, 8613.
27. Tantishaiyakul, V.; Worakul, N.; Wongpoowarak, W. Int J Pharm 2006, 325, 8.
28. Mathiowitz, E.; Amato, C.; Dor, P.; Langer, R. Polymer 1990, 31, 547.
29. Sheiko, S.; Frey, H.; Moller, M. Colloids Polym Sci 1992, 270, 440.
30. Göpferich, A.; Langer, R. J Polym Sci Part A: Polym Chem 1993, 31, 2445.
31. Göpferich, A.; Tessmar, J. Adv Drug Deliv Rev 2002, 54, 911.
32. Lahrouni, A.; Arman, J. Eur Polym J 1995, 31, 347.